Tectonics

RESEARCH ARTICLE
10.1029/2020TC006517

Key Points:

- The sub-Cretaceous unconformity in the southern Colorado Plateau can be explained by flexural uplift of the northern flank of the Bisbee Rift system
- Flexure of the rift flank also resulted in an outer low or depositional trough in the Four Corners region of the plateau
- The anomalous thickness of the Morrison Formation in the Four Corners region is related to constructive flexural interference between a back-bulge depozone related to the Sevier thrust belt and a flexural trough related to rift flank flexure

Correspondence to:
J. B. Chapman,
jay.chapman@uwyo.edu

Citation:
Chapman, J. B., & DeCelles, P. G. (2021). Beveling the Colorado Plateau: Early Mesozoic rift-related flexure explains erosion and anomalous deposition in the southern Cordilleran foreland basin. *Tectonics*, *40*, e2020TC006517. https://doi.org/10.1029/2020TC006517

Received 14 SEP 2020
Accepted 21 MAY 2021

Beveling the Colorado Plateau: Early Mesozoic Rift-Related Flexure Explains Erosion and Anomalous Deposition in the Southern Cordilleran Foreland Basin

James B. Chapman[1] **and Peter G. DeCelles**[2]

[1]Department of Geology and Geophysics, University of Wyoming, Laramie, WY, USA, [2]Department of Geosciences, University of Arizona, Tucson, AZ, USA

Abstract Deposition of the Late Jurassic Morrison Formation in a back-bulge depozone and formation of the overlying sub-Cretaceous unconformity above a forebulge mark the birth of the foreland basin system in the central U.S. Cordillera. In the southern U.S. Cordillera, the Morrison Formation is either anomalously thick or absent and the sub-Cretaceous unconformity cuts out progressively older stratigraphy toward the south on the Colorado Plateau. Based on results of 2D and 3D flexural modeling, we suggest that flexural uplift of the northern rift flank of the Bisbee segment of the Borderland Rift Belt can explain these observations. Structural restoration of the sub-Cretaceous unconformity indicates a minimum of 1.5 km of uplift and flexural models with an effective elastic thickness of 55 ± 5 km can reproduce the geometry of the unconformity and rift flank. This implies that effective elastic thickness has decreased between the Jurassic and the present, consistent with hypotheses for uplift and modification of the Colorado Plateau lithosphere during the Late Mesozoic to Cenozoic. Modeling results also predict the presence of a rift-related flexural trough in the Four Corners region of the Colorado Plateau, which may explain above-average thickness of the Morrison Formation. Constructive interference between a flexural back-bulge depozone and a flexural rift-flank trough may help explain anomalously high Late Jurassic subsidence.

Plain Language Summary Continental rifting in southern Arizona during the Jurassic caused the margins of the rift system to be flexed upward and eroded. The erosion resulted in a regionally extensive, low-angle unconformity beneath Cretaceous sedimentary rocks in the southern Colorado Plateau. As the rift margin was flexed upward it caused nearby parts of the rigid crust to flex downward in response, specifically in the Four Corners region of the Colorado Plateau (approximately where the state boundaries of Arizona, New Mexico, Colorado, and Utah meet). The downward flexure in the Four Corners area created a basin where sediments of the Morrison Formation accumulated and are thicker than anywhere else in the western U.S.

1. Introduction

Sedimentation patterns in foreland basin systems provide some of the best constraints on the tectonic histories of Cordilleran-style orogens and are the basis for evaluating a wide range of geodynamic models (e.g., Beaumont, 1981; Dávila et al., 2010; DeCelles & Horton, 2003; Liu & Gurnis, 2010; Miall & Catuneanu, 2019; Painter & Carrapa, 2013). The Mesozoic to early Cenozoic Western Interior Basin is an archetypal retroarc foreland basin system and informs much of the current thinking about Cordilleran systems globally and throughout geologic time (DeCelles, 2004; Jordan, 1981; Kauffman & Caldwell, 1993; Miall & Catuneanu, 2019; Plint et al., 2012). In the central and northern U.S. Cordillera, the onset of deformation in the Cordilleran thrust belt and sedimentation in the eastward adjacent foreland basin system are primarily constrained by deposition of the upper Jurassic Morrison Formation (Figure 1) in what has been interpreted to be the deposits of a back-bulge depozone (DeCelles & Curie, 1996; Fuentes et al., 2009). Supporting this hypothesis is a regionally extensive disconformity that separates the Morrison Formation from overlying Aptian (125–113 Ma) sedimentary rocks and is interpreted to have formed during the passage of a flexural forebulge possibly combined with dynamic uplift (Currie, 1998; DeCelles et al., 2004). Although this interpretation is consistent with stratigraphic data from southern Utah to Alberta (DeCelles, 2004; Miall et al., 2008), it does not explain regional stratigraphic relationships in the southern Colorado Plateau and

10.1029/2020TC006517

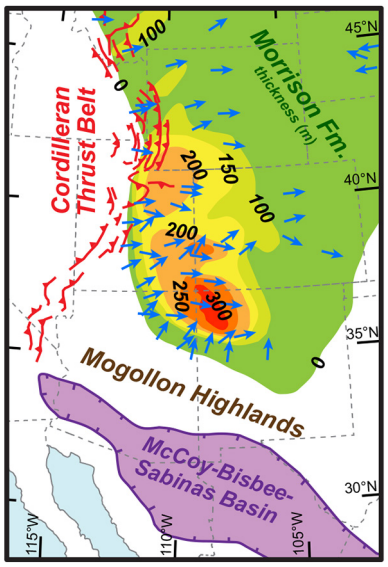

Figure 1. Overview map of the central and southern U.S. Cordillera showing thickness and paleocurrent directions (blue arrows) for the Morrison Formation (deposited 156–147 Ma). The Borderland Rift belt comprises the McCoy, Bisbee, Chihuahua, and Sabinas rift basins, which contain syn-rift deposits (ca. 156–150 Ma) similar in age to the Morrison Formation. Data sources: Craig et al. (1955), Cadigan, (1967), Dam et al. (1990), Turner and Fishman, (1991), DeCelles (2004), and Heller et al. (2015).

regions to the south, where the sub-Cretaceous disconformity becomes a very low-angle angular unconformity that bevels progressively older strata to the south, cutting down-section into lower Paleozoic and Proterozoic rocks in central Arizona and New Mexico. The amount of missing stratigraphic section in this region (ca. 2 km) is incompatible with eustastic changes or the magnitude of erosion associated with uplift of a flexural forebulge (DeCelles & Burden, 1992).

An alternative model to explain the sub-Cretaceous unconformity in the southern Colorado Plateau region is uplift of the northern flank of the Late Jurassic to Early Cretaceous Border (Bisbee) rift belt (Figure 1) (Bilodeau, 1986; Dickinson, 2013; Dickinson et al., 1989). This study investigates whether flexural uplift of the northeast Bisbee rift shoulder (defined as the gently sloping outer flank of the rift highland; Şengör, 2011) is a viable mechanism to explain the geometry of the sub-Cretaceous unconformity and explores potential interference patterns between distal foreland basin-related flexure and rift-related flexure. To model lithospheric flexure, we constructed a pre-Cretaceous paleogeologic (subcrop) map for the Colorado Plateau region (Figure 2) and used the Jurassic-Cretaceous unconformity as a datum or geometric marker. Flexure was modeled analytically in two-dimensions (2D) and numerically in both 2D and three-dimensions (3D) with spatially variable loads and effective elastic thickness.

2. Geologic Background

2.1. Stratigraphy

For the purposes of this study, the pre-Cretaceous stratigraphy of the Colorado Plateau and southern U.S. Cordillera is divided into several units, including the Precambrian basement (predominantly Proterozoic igneous and metamorphic rocks of the Yavapai and Mazatzal lithospheric provinces), Cambrian through Permian sedimentary rocks, the Triassic Moenkopi and Chinle Formations, the Triassic-Jurassic Glen Canyon Group, the middle Jurassic San Rafael Group, and the upper Jurassic Morrison Formation. The middle Jurassic (172–155 Ma) San Rafael Group is located stratigraphically beneath the Morrison Formation and was deposited throughout the southern U.S. Cordilleran foreland (Anderson & Lucas, 1994; Dickinson & Gehrels, 2008). The San Rafael Group crops out in the Colorado Plateau region and correlative rocks, mainly eolian sandstone, are exposed in southern Arizona and northern Sonora, Mexico (González-León et al., 2009; Lawton et al., 2018; Riggs et al., 1993) suggesting the presence of a semi-continuous depositional surface.

In the central U.S. Cordillera, the Morrison Formation is generally <250 m thick, except in the Four Corners region of the Colorado Plateau where it reaches >300 m (Craig et al., 1955; Dam et al., 1990, Figure 1). The Morrison Formation is notable for its symmetric, saucer-like isopach pattern, which contrasts with typical foredeep deposits that thicken exponentially toward the thrust belt (Heller et al., 1986). The symmetrically shaped Morrison lithosome has been interpreted to be a back-bulge depozone within a flexural foreland basin system (Figure 2) and to represent the oldest stratigraphic evidence for the retroarc thrust belt (DeCelles & Burden, 1992; DeCelles & Currie, 1996; Currie, 1998; Fuentes et al., 2009). Sediment provenance and paleocurrent data support this interpretation (Craig et al., 1955; Currie, 1998; DeCelles & Burden, 1992; Dickinson & Gehrels, 2008; Heller et al., 2015; Robinson & McCabe, 1997; Turner & Fishman, 1991). An age-equivalent foredeep depozone related to the Morrison Formation is absent, presumably eroded, and has been called the phantom foredeep for its inferred presence (Long, 2012; Royse, 1993). Radiometric ages of tuffs in the Morrison Formation and magnetostratigraphic studies indicate that it was deposited between ca. 156 and 147 Ma (Kowallis et al., 1998; Maidment & Muxworthy, 2019; Trujillo et al., 2014; Turner & Peterson, 2004). The uppermost part of the Morrison Formation is marked by a several tens of meters thick composite paleosols (Currie, 1998; Demko et al., 2004) and a major Late Jurassic–Early Cretaceous disconformity or paraconformity called the "K unconformity" by Pipiringos and O'Sullivan (1978); this will be

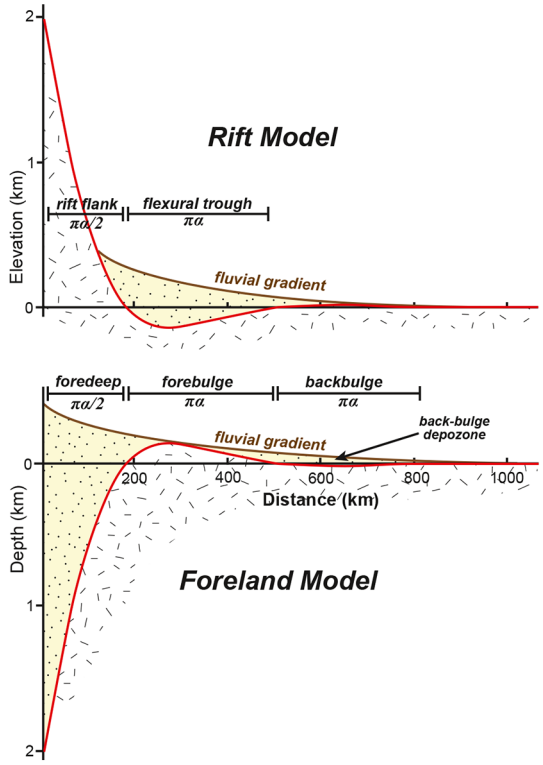

Figure 2. Schematic diagram illustrating basins (yellow stippled areas located beneath the fluvial gradient) formed by flexure of the lithosphere in rift systems and in foreland basin systems. The two flexural profiles are mirror images of each other and are analytical solutions to flexure of a "broken" plate (Turcotte & Schubert, 2002). The models were constructed using an effective elastic thickness of 40 km. In the rift model, the upward directed force is supplied by unloading of the crust by normal faulting (Weissel & Karner, 1989). In the foreland model, the downward directed force is supplied by loading the crust with a retroarc thrust belt (DeCelles & Giles, 1996; DeCelles, 2012). The wedge top depozone is not shown in the foreland model (cf., DeCelles & Giles, 1996). In most of the North American Cordillera, the Morrison Formation is interpreted to have been deposited in a back-bulge depozone (DeCelles & Curie, 1996). This study proposes that part of the Morrison Formation in the Four Corners region of the Colorado Plateau was also deposited in the flexural trough rift basin. The width of the back-bulge depozone and the flexural trough are related to the flexural parameter α (Turcotte & Schubert, 2002).

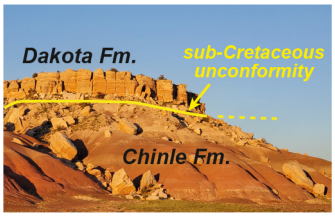

Figure 3. Photograph of the sub-Cretaceous unconformity above the Triassic Chinle Formation, taken ~25 km north of the town of St. Johns, Arizona.

referred to as the sub-Cretaceous disconformity herein. The lacuna represented by the sub-Cretaceous disconformity spans an estimated 20 Myr and has been interpreted to be related to extreme stratigraphic condensation during the eastward migration of the flexural forebulge bounding the west side of the Morrison back-bulge depozone (Currie, 1997, 1998; DeCelles & Currie, 1996).

DeCelles (2004) modeled the shape and position of the Morrison depocenter using the Turcotte and Schubert (2002) analytical solution for 2D flexure of a broken plate (Figure 2), showing that loading of the lithosphere by the Late Jurassic to Early Cretaceous Luning-Fencemaker thrust belt (Oldow, 1984; Wyld, 2002), a westward precursor to the Sevier thrust belt, reproduced the geometry and position of the Morrison lithosome with a flexural rigidity of 10^{24} Nm (~53 km effective elastic thickness). The flexural modeling predicts ≤10 m of subsidence in the back-bulge region, however, dynamic subsidence in the Cordilleran retroarc region (Gurnis, 1992) could have pulled down the entire load-driven flexural profile, allowing thicker back-bulge deposits to develop (e.g., Catuneanu, 2004; DeCelles, 2012). When combined with an aggradational fluvial gradient extending from the thrust belt across the crest of the forebulge to the craton (Figure 2), >150 m of Morrison Formation could have accumulated in the back-bulge region (Currie, 1998; DeCelles, 2004). The flexural modeling also suggested that the forebulge may have had as much as 300 m of positive relief above the regional datum, consistent with the formation of the sub-Cretaceous disconformity above the Morrison Formation.

Overlying the Morrison Formation and the sub-Cretaceous disconformity are Aptian-Albian (ca. 125–100 Ma) sedimentary units, including the Kootenai, Cloverly, Cedar Mountain, Kelvin, Lakota, and Burro Canyon Formations (Currie et al., 2012; Laskowski et al., 2013; Ludvigson et al., 2010; Owen, 1973; Painter et al., 2014; Sprinkel et al., 2012; Tschudy et al., 1984). The Dakota Formation, also known as the Dakota Group or Dakota Sandstone, disconformably overlies the lower Cretaceous units. The unconformity beneath the Dakota Formation is called the sub-Dakota unconformity (e.g., Dickinson, 2013). In most areas, the sub-Dakota unconformity (middle Cretaceous in age) is distinct from the sub-Cretaceous disconformity (early Cretaceous in age; ca. 145–120 Ma; Currie et al., 2008, 2012). However, in southwest Utah, Arizona, and southern New Mexico the lower Cretaceous sedimentary rocks (e.g., Burro Canyon Formation) are absent and the two unconformities are co-located (Figure 3). This study examines the sub-Cretaceous disconformity and the role of flexure during deposition of the Morrison Formation during the Jurassic. The Dakota Formation was deposited in a foredeep depozone and transitions up-section from fluvial/estuarine to shallow-marine strata (e.g., Currie, 1998; Currie et al., 2008; Sprinkel et al., 2012; Ulicny, 1999). In the southern Colorado Plateau region, the Dakota Formation onlaps southward onto the Mogollon Highlands and is time-transgressive, but generally Albian-Cenomanian (ca. 105–95 Ma) in age (Cobban & Hook, 1984; Currie, 1998; Williamson et al., 1993).

2.2. Mogollon Highlands and Bisbee Rift System

The Cordilleran foreland basin system was bounded on the south by the Mogollon Highlands, an approximately southeast-northwest trending

paleo-topographic high interpreted to have been the uplifted northern rift shoulder of the Bisbee rift system (Bilodeau, 1986; Dickinson et al., 1989; Dickinson & Lawton, 2001; Lawton et al., 2020). Paleocurrent, provenance, and geochronologic data suggest that the northeast rift shoulder was a major source of sediment to the Morrison and Dakota Formations (Cadigan, 1967; Craig et al., 1955; Dickinson & Gehrels, 2008; Hansley, 1986; Turner-Peterson, 1986; Turner & Fishman, 1991). During deposition of the Morrison Formation, the Mogollon Highlands and Mogollon slope were erosional surfaces incised by north- to northeastward flowing streams and rivers (Aubrey, 1989; Bilodeau, 1986). Sediment provenance data indicate that, at least locally, the Paleozoic sedimentary cover had been stripped off the Mogollon Highlands and that Proterozoic basement was exposed by Late Jurassic time (Dickinson & Gehrels, 2008; Laskowski et al., 2013). During the middle to Late Cretaceous the Mogollon Highlands and slope were onlapped by the Dakota Formation and equivalent rocks. Pre-Dakota or pre-Cretaceous paleogeologic ("subcrop") maps show that progressively older stratigraphic units are exposed beneath the unconformity closer to the Mogollon Highlands (Dickinson, 2013; Dickinson et al., 1989; this study) (Figure 4). This study investigates potential uplift of the Mogollon Highlands during the deposition of the Morrison Formation during the Jurassic (ca. 155–145 Ma). The Morrison Formation marks the beginning of uplift and erosion of the Mogollon Highlands (Dickinson & Gehrels, 2008; Turner & Fishman, 1991; Turner-Peterson, 1986). Where the Morrison Formation was not deposited, south of ~34°N latitude (present-day coordinates), age-equivalent uplift of the Mogollon Highlands is marked by the sub-Dakota unconformity. Onlap of the Dakota Formation (as young as ~94 Ma) onto the Mogollon highlands, therefore, constrains the duration of this specific uplift event. Renewed uplift of the Mogollon Highlands may have continued after the Jurassic, including during the Laramide orogenic event (ca. 80–40 Ma) (Chapman et al., 2019; Gastil et al., 1992; Karlstrom et al., 2020), but later periods of uplift are not related to the deposition of the Morrison Formation, the sub-Cretaceous disconformity, or the sub-Dakota unconformity.

The 2–3 km thick Bisbee rift basin is part of the larger Borderland rift belt that also includes the McCoy, Chihuahua, and Sabinas basins (Dickinson & Lawton, 2001) (Figure 1). The Borderland rift belt has been interpreted as a back-arc rift related to Farallon slab roll-back and the opening of the Gulf of Mexico (Lawton & McMillan, 1999; Stern & Dickinson, 2010) in a highly oblique (nearly neutral) plate kinematic framework (DeCelles, 2004). The Late Jurassic to middle Cretaceous Bisbee basin overlaps in age with the Morrison Formation (Figure 5). Paleontological data and radiometric dates from the oldest, syn-rift, basal members of the Bisbee Group are 156–150 Ma (Kluth et al., 1982; Olmstead & Young, 2000; Spencer et al., 2011), which demonstrates that Bisbee basin rifting and Morrison deposition were synchronous. Post-extensional thermotectonic subsidence of the Bisbee rift basin commenced during the Early Cretaceous (ca. 130 Ma) and waned during the Albian (ca. 100 Ma) when marine limestone was deposited in the rift basin (Dickinson & Lawton, 2001).

3. Methods and Results

3.1. Paleogeologic (Subcrop) Map Patterns

The Late Jurassic topography and geometry of the Mogollon Highlands and Bisbee rift shoulder have been obscured by subsequent processes including Late Cretaceous to Paleogene deformation related to the Laramide orogenic event and Basin-and-Range extension during the Neogene. We use the position of the Bisbee basin as a proxy for the position of the Bisbee rift and use the sub-Dakota unconformity as a proxy for the topographic surface during and immediately after rifting.

First, we constructed a subcrop map beneath the sub-Dakota unconformity for the Colorado Plateau region and southern U.S. Cordillera (Figure 4) using 1:48,000 to 1:250,000 geologic maps. This map is similar to an existing "sub-Dakota" paleogeologic map made by Dickinson (2013), Dickinson et al. 1989 and includes data from parts of the Rio Grande rift, Colorado Plateau transition zone, and the periphery of the Basin-and-Range province. Stratigraphic units were only mapped where the sub-Dakota unconformity is present (i.e., where the Dakota Formation or other lower Cretaceous rocks are not eroded). Stratigraphic units intersecting the subcrop surface are older southward and their contacts strike sub-parallel to the margin of the Bisbee basin, which suggests that the dip of strata was northeastward, perpendicular to the Bisbee basin margin during erosion.

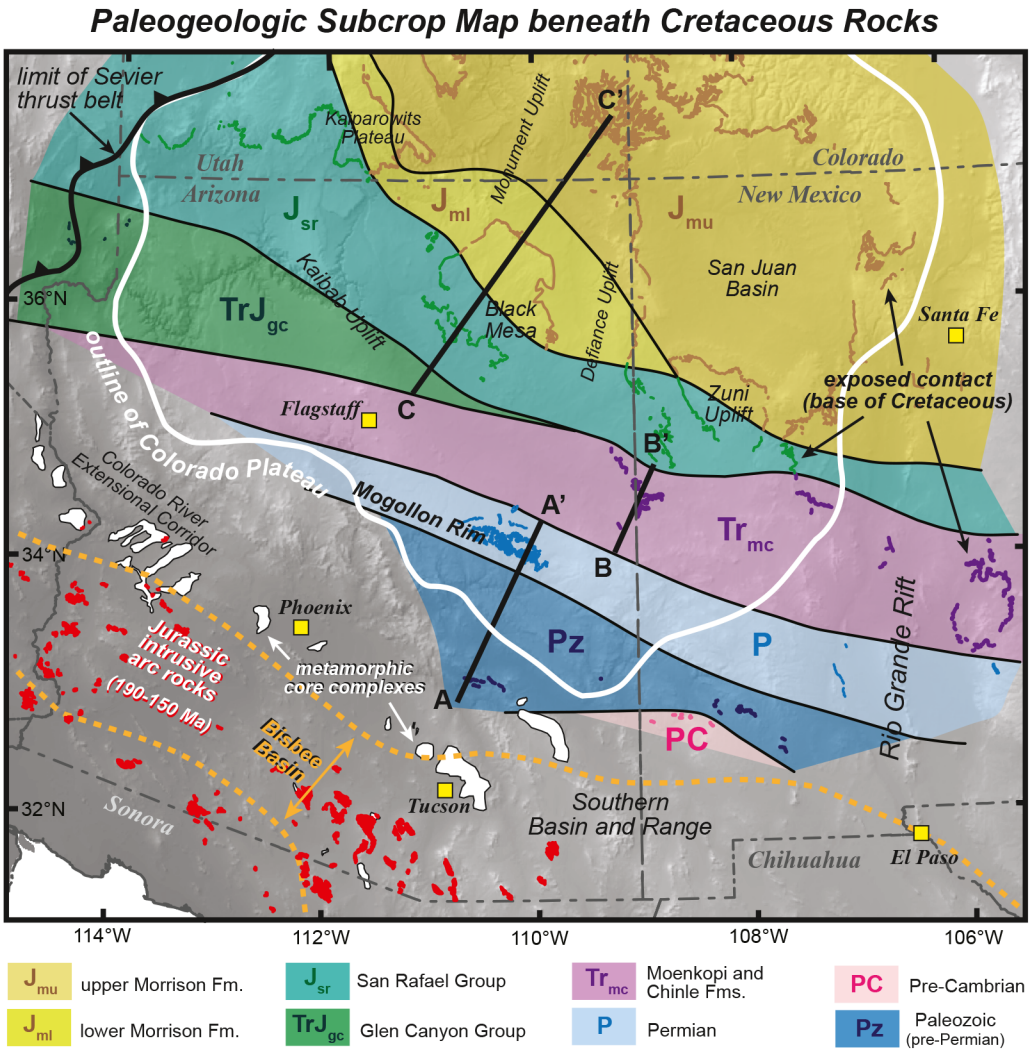

Figure 4. Paleogeologic ("subcrop") map beneath the sub-Cretacous unconformity. More darkly shaded lines within each map unit are the actual data used to construct the map. The division between the upper and lower Morrison Formation is adopted from Dickinson (2013). Ages of Jurassic arc rocks are from Barth et al. (2008, 2017) and Tosdal and Wooden (2015). Syn-rift deposits in the Bisbee basin are ca. 156–150 Ma and basin fill deposits are as young as ca. 100 Ma (Dickinson & Lawton, 2001; Spencer et al., 2011).

Next, we constructed a cross-section from the Transition Zone in southern Arizona to the Four Corners area of the Colorado Plateau using structural data and unit thicknesses from previously published geologic maps (Figure 6). The cross-section was initially constructed with no vertical exaggeration perpendicular to the trend of the stratigraphic contacts in the subcrop map and has two lateral offsets (A′-to-B and B′-to-C) that were chosen to capture areas with the most data coverage. The cross-section was then restored by removing folding and faulting, chiefly extension related to normal faulting, and then flattening on the sub-Dakota unconformity. Vertical exaggeration was then added to the cross-section to make stratigraphic units and very low-angle structural relationships visible (Figure 6). Assuming that stratigraphic units maintained their thicknesses southward before erosion, the initial restoration suggests ~1.5 km of structural relief (i.e., ~1.5 km of eroded stratigraphic section). Paleocurrent data from fluvial strata in the Dakota Formation in the vicinity of the cross-section (Owen, 1973) demonstrate that the sub-Dakota unconformity surface (base of Dakota Formation or lower Cretaceous rocks) was not flat, but sloped downward to the north and northeast from the Mogollon Highlands. Although the topographic relief and geometry of this fluvial surface during the Late Jurassic are unknown, we estimated it using an ideal equilibrium river profile with standard concavity parameters (Hack, 1975; Whipple & Tucker, 1999) and assumed 1 km topographic relief

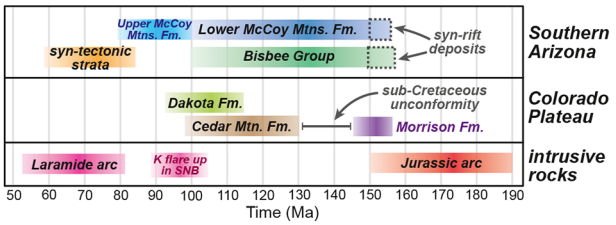

Figure 5. A timeline showing the age of sedimentary units and intrusive igneous rocks in southern Arizona and the age of sedimentary rocks deposited on the Colorado Plateau. Data sources: pink = Laramide arc (Seedorff et al., 2019) and Cretaceous (K) flare up timing in the Sierra Nevada batholith (SNB) (Kirsch et al., 2016); orange = syn-tectonic strata associated with the Laramide Orogeny (Clinkscales & Lawton, 2018; Caylor et al., 2021; Dickinson et al., 1989), blue = McCoy Mountains Formation (Barth et al., 2004; Spencer et al., 2011), dark green = Bisbee Group (Dickinson & Lawton, 2001; Kluth, 1982; Olmstead & Young, 2000), light green = Dakota Formation (Cobban & Hook, 1984; Williamson et al., 1993), brown = Cedar Mountain Formation, also includes other lower Cretaceous units (e.g., Burro Canyon Formation) (Ludvigson et al., 2010), purple = Morrison Formation (Kowallis et al., 1998; Maidment & Muxworthy, 2019; Trujillo et al., 2014; Turner & Peterson, 2004), red = Jurassic arc (Barth et al., 2008, 2017; Tosdal & Wooden, 2015).

over the ~550 km length of the restored cross-section, consistent with gradients of moderately sized river systems (Sklar & Dietrich, 1998). Our estimate of paleo-topographic relief is conservative, falling in the lower range of global continental rift flank topographic relief (1–4 km; Chéry et al., 1992), and is similar to the amount of relief observed on the flanks of the Rhine graben and Rio Grande rift (Brown & Phillips, 1999; Villemin et al., 1986), which have dimensions similar to those of the Bisbee rift segment. The sum of structural relief and topographic relief suggests ca. 2.5 km of total uplift of the northern Bisbee rift shoulder.

3.2. Flexural Modeling

The asymmetric, concave-up geometry of rift shoulders is a classic flexural isostatic response to unloading (upward-directed vertical force) of the lithosphere and mirrors the flexural response to loading (downward-directed vertical force) of the lithosphere (Stern & ten Brink, 1989; Weissel & Karner, 1989) (Figure 2). In comparison to flexural profiles of foreland basin systems (DeCelles & Giles, 1996), the rift flank is analogous to the foredeep and the flexural trough is analogous to the forebulge. Flexural troughs in rift systems have also been referred to as "outer lows" and "hinterland basins" (ten Brink & Stern, 1992; van Balen et al., 1995). The upward-directed force in rift systems is a combination of positively buoyant forces that result from erosion, normal faulting, thermal expansion of the crust, and thinning of the mantle lithosphere, and negatively buoyant forces that result from sedimentation, crustal thinning, crustal metamorphism, and basaltic underplating/intrusion (Chéry et al., 1992; Mueller et al., 2009; van der Beek et al., 1994; Weissel & Karner, 1989). The magnitudes of the forces resulting from these individual processes during the Late Jurassic is unknown and in the following models, only the total magnitude of the upward-directed force (sum of all sub-forces) is considered. Likewise, we do not consider rift flank flexure/uplift related to processes such as small-scale convection (Buck, 1986; van Wijk, Lawrence, & Driscoll, 2008; van Wijk, Van Hunen, & Goes, 2008) or mantle flow and dynamic topography (Daradich et al., 2003), although these processes could theoretically have contributed to the total load experienced by the elastic portion of the lithosphere.

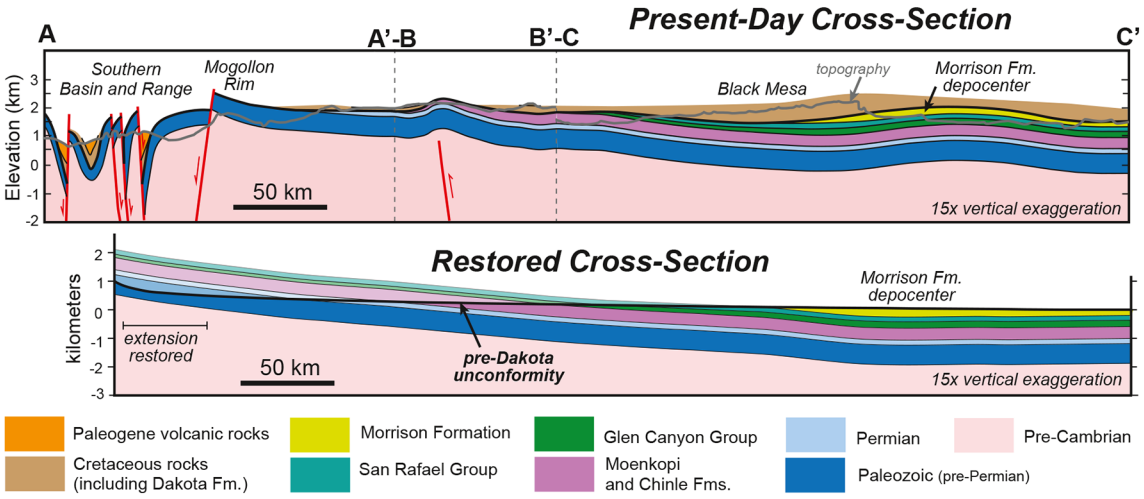

Figure 6. (Top panel) Present-day cross section showing the thickness and geometry of sedimentary cover on the southern Colorado Plateau and transition zone. Cross-section location shown in Figure 2. Bottom panel) Structural restoration of the cross-section to Late-Jurassic time (time of Morrison Formation deposition). The restored cross-section is line length balanced. The very high vertical exaggeration distorts the lengths of the sedimentary units in the southern Basin and Range area such that they appear longer than they are in the non-exaggerated section. See text for details of restoration.

In addition to the magnitude of the vertical load, the two other main variables that control the geometry of flexural profiles are horizontal forces and flexural rigidity. Forces related to horizontal stresses, sometimes called "tectonic" or "buckling" forces, are often ignored in flexural modeling and when they are considered, it is generally only in contractional systems (e.g., Martinod & Davy, 1992; Tikoff, and Maxson, 2001). We ignore horizontal forces for the following models. We express flexural rigidity as effective elastic thickness using a Young's modulus of 70 GPa and a Poisson's ratio of 0.25.

3.2.1. 2D Models

To model flexure in 2D, we used the restored geometry (lower panel in Figure 6) of the top of the Jurassic San Rafael Group (base of the Morrison Formation). The Morrison Formation is not believed to have been deposited south of ca. 34°N latitude whereas rocks (mainly eolian sandstone) correlative with the San Rafael Group crop out locally throughout southern Arizona and northern Sonora, Mexico (González-León et al., 2009; Lawton et al., 2018) suggesting the presence of a semi-continuous depositional surface. We treat the top of the San Rafael Group as a paleo-horizontal surface prior to rifting.

First, we employ the analytical solution of Weissel and Karner (1989) for elastic flexure related to rifting (Figure 7). This model solves the equation for 2D flexure of a plate analytically by treating the vertical force as a line load (approximated using the amount of heave on a planar normal fault) and assuming a constant effective elastic thickness. This class of model is a "broken" lithosphere model in which the second derivative (bending moment) of vertical displacement with respect to distance at the position of the line load is equal to zero. By contrast, the slope (first derivative) is equal to zero at the position of the line load for "continuous" or "intact" lithosphere models. We prescribed a fault dip of 60° (assuming Andersonian normal faulting), an upper mantle density of 3300 kg/m^3, a basin fill density of 2600 kg/m^3, and we varied the fault heave and effective elastic thickness to match the restored San Rafael Group surface. Acceptable fits to the data (estimated visually) are obtained using an effective elastic thickness of 80 $\pm$ 5 km and a fault heave of 2650 $\pm$ 50 m (Table 1). The best model produced a flexural trough ~500 km wide, located ~550 km away from the edge of the vertical load, and ~150 m deep (Figure 7). To model the flexure of an "intact" plate, we used the analytical solution for 2D flexure from Turcotte and Schubert (2002). Similar to before, we varied the vertical line load and effective elastic thickness to match the restored San Rafael Group surface. An effective elastic thickness of 50 $\pm$ 5 km and an upward-directed line load of 3.5 $\pm$ 0.5 $\times$ 10^{12} N/m resulted in the closest match (visually estimated) between modeled flexural profile and the geometry of the restored San Rafael Group surface (Table 1). The best "intact" model produced a flexural trough ~400 km wide, located ~525 km away from the edge of the vertical load, and ~80 m deep.

Vertical line loads and constant effective elastic thickness are likely not realistic conditions for the flexure of rift flanks. In our next model, we used spatially variable loads and flexural rigidity using a 2D centered finite-difference (numerical) solution from Chapman et al. (2017), which is a "continuous" lithosphere model (Figure 7). Mueller et al. (2009) suggested that two of the most important loads in rift systems are the replacement of crust with mantle during crustal thinning (downward-directed load due to +400 kg/m^3 density difference) and the replacement of mantle lithosphere with asthenospheric mantle (upward-directed load due to −100 kg/m^3 density difference). Following this approach, we prescribed 10 km of crustal thinning and varied the magnitude of mantle lithosphere replacement/thinning for a 100 km rectangular region beneath the rift, which is the approximate width of the Bisbee basin. We prescribed an effective elastic thickness of 15 km beneath the rift region and varied the effective elastic thickness of the adjacent Colorado Plateau region. The closest match (visually estimated) between the modeled flexural profile and the restored San Rafael Group surface was achieved using an effective elastic thickness of 55 $\pm$ 5 km and 50 $\pm$ 5 km vertical thinning of the mantle lithosphere (Table 1). The best model produced a flexural trough ~250 km wide, located ~525 km away from the edge of the vertical load, and ~65 m deep.

3.2.2. 3D Model

Lastly, we modeled flexure in 3D with spatially variable loads using a second-order finite-difference numerical approximation modified from Cardozo and Jordan (2001) (Figure 8). This model is a "continuous" plate model. The purpose of the 3D model was not to match the restored geometry of the San Rafael Group, but to investigate the interaction of lithospheric flexure in the distal Cordilleran foreland basin with flexure related to the Bisbee rift. We used the results of the 2D models to constrain the 3D model geometry and

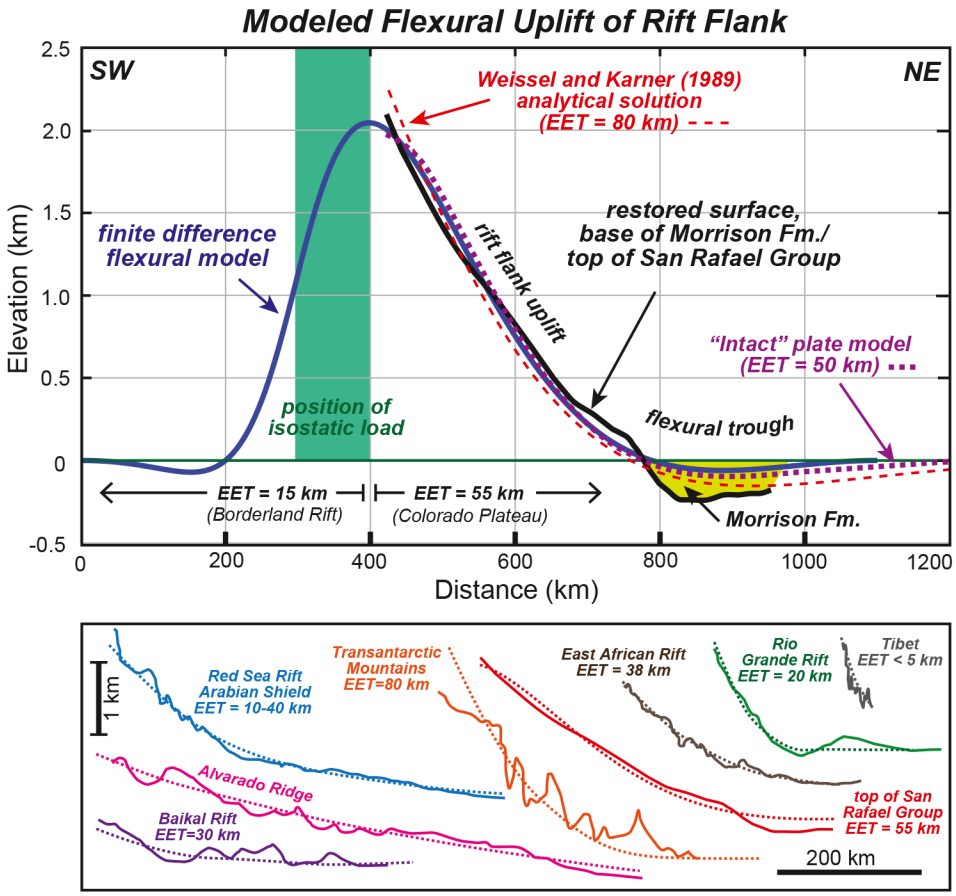

Figure 7. (Top panel) Results of analytical and numerical 2D flexural modeling. Models were evaluated on their ability to reproduce the restored geometry of the top of the San Rafael Group (base of Morrison Formation) show in the bottom panel in Figure 6. Modeling parameters and results are also listed in Table 1. Bottom panel) Topographic profiles (solid lines) and fitted flexural models (dashed lines) for rift flanks from a variety of rift systems globally to compare against the results of the 2D flexural model of the top of the San Rafael Group (red lines) presented in the top panel. EET = effective elastic thickness. The Alvarado Ridge is not a rift flank, but an example of a tilted surface produced by epeirogenic uplift that is presented for comparison (Eaton, 2008; Roy et al., 1999). Data sources: Baikal rift (van der Beek, 1994); Red Sea rift (Chen et al., 2015); Transantarctic Mountains (ten Brink et al., 1997), East African Rift, Lake Albert area (Ebinger et al., 1989, 1991), Rio Grande rift, Tularosa Basin area (Peterson & Roy, 2005), Tibet (Masek et al., 1994).

parameters. A homogenous effective elastic thickness of 55 km was employed to be consistent with our 2D finite difference modeling and the results of DeCelles (2004) for the Morrison basin. The vertical load related to the Bisbee rift was modeled with a 100 km wide by 750 km long parallelogram located in the geographic position and orientation of the Bisbee basin (Figure 8) with an upward-directed stress of ca.

Table 1
Results of Flexural Modeling

	Best fit effective elastic thickness (km)	Width of flexural trough (km)	Depth of flexural trough (m)	Distance from edge of rift flank to center of flexural trough (km)
Broken lithosphere, analytical solution (2D)	80 ± 5	500	150	550
Intact lithosphere, analytical solution (2D)	50 ± 5	400	80	525
Finite-difference flexural model (2D)	15–55	250	65	525
Finite-difference flexural model (3D)	55	~475	60–70	~425

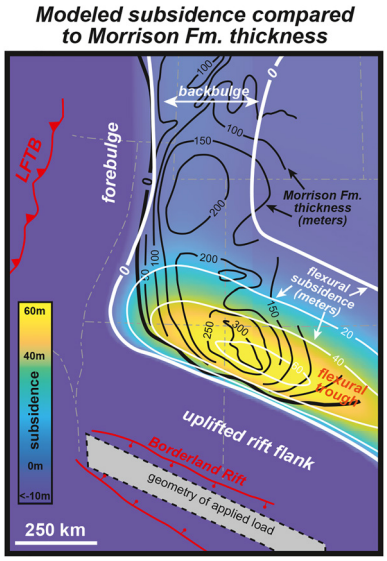

Figure 8. Results of 3D flexural modeling that include flexure related to the Bisbee rift flank and flexure related to the Cordilleran foreland basin system. Colors and white contours represent modeled subsidence, black contours are the thickness of the Morrison Formation from Figure 1.

49 MPa applied to match the amount of flexure generated by the line loads in 2D models.

Previous flexural modeling of the Cordilleran foreland basin system during deposition of the Morrison Formation (DeCelles, 2004) used a "broken" plate model, which cannot be easily combined with the 3D "continuous" plate model. We employed two different methods to work around this obstacle, which yielded nearly identical results. For the first method, we simultaneously modeled loading from the Cordilleran thrust belt and Bisbee rift, but moved the position of the thrust belt load westward until the position of the back-bulge depozone matched the location of the Morrison basin. We used the vertical topographic load employed by DeCelles (2004), a rectangle with dimensions 1.5 km high by 160 km wide with a density of 2700 kg/m^3, and extended it 1500 km in the third dimension (oriented north-south) to create a block that approximates the geometry of the load related to the Cordilleran thrust belt. The center of the load was positioned ~1000 km west of the center of the Morrison basin to match the back-bulge position. For comparison, the central position of the thrust belt load in the DeCelles (2004) model was located ca. 750 km west of the Morrison basin center.

The second method we used was to take the "broken" plate 2D flexural profile from DeCelles (2004), extend it north-south to make a 3D flexural surface, and then add it to the flexural surface produced by modeling of the Bisbee rift alone. The results of this second method are shown in Figure 8. Results from both methods show constructive interference between subsidence related to the back-bulge depozone and subsidence related to the rift-controlled flexural trough. Maximum subsidence in the back-bulge region is 5–10 m and maximum subsidence in the flexural trough is 60–70 m, and both values are consistent with the 2D modeling. The maximum amount of modeled subsidence is located in the Four Corners region of the Colorado Plateau, coincident with the maximum thickness of the Morrison Formation (Figure 8).

4. Discussion

The two variables we explored in the flexural models are vertical load and effective elastic thickness. Only the effective elastic thickness results are geologically meaningful because of the poor constraints on total uplift/flexure of the rift shoulder as inferred from the geometry of the top of San Rafael Group surface during the Late Jurassic. Although our cross-section restoration (to Late Jurassic time) indicates ca. 1.5 km of structural relief, the topographic relief of this surface is based only on geologically reasonable values of modern river gradients and modern rift flank topography. Our estimates of topographic relief are conservative and thus the vertical load estimates in the best fit models could be considered rough minimum estimates, but we caution against overinterpretation. Furthermore, the ways in which vertical forces were calculated are non-unique and likely not geologically significant. For example, our best-fit 2D model using the Weissel and Karner (1989) method suggests ~2650 m of fault heave, which is similar in magnitude to both the thickness of the Bisbee basin fill (2–3 km) and our estimate for total rift shoulder uplift (2.5 km), but this almost certainly does not represent slip on an actual fault plane or fault system—it is merely the result of a geometric expression used to calculate a total vertical load. Similarly, our estimates of crustal and mantle thinning in the 2D finite-difference model are only used as a guideline to calculate the total vertical load and may not have any geologic significance.

Conversely, we do ascribe geologic importance to our estimates of effective elastic thickness. The wavelength of elastic flexure is independent of the magnitude of the vertical load and fully dependent on flexural rigidity. The effective elastic thickness of our best-fit 2D finite-difference models for flexure of the Bisbee rift flank (55 ± 5 km) overlaps within uncertainty the previous estimate (~53 km) based on flexure of the Cordilleran foreland basin (DeCelles, 2004). The effective elastic thickness of the modern Colorado Plateau

is ca. 40 km in the center of the plateau and decreases to ca. 20 km on the margins (Lowry et al., 2000). If the results of our modeling are accurate, they suggest that the effective elastic thickness has decreased between the Late Jurassic and the present-day. There are multiple possible explanations for the decrease in effective elastic thickness. The continental mantle and portions of the lower crust may have foundered or delaminated from the base of the Colorado Plateau (e.g., Levander et al., 2011). The mantle lithosphere may have been thermally eroded by small-scale mantle convection (e.g., van Wijk et al., 2010) or asthenospheric upwelling (e.g., Karlstrom et al., 2008, 2012; Moucha et al., 2009). The continental mantle and lower crust may have been metasomatically weakened (e.g., hydration) during low-angle subduction (e.g., Feucht et al., 2017; Humphreys et al., 2003; Jones et al., 2015). This study cannot distinguish between these processes, which are all proposed to have occurred during the Cenozoic, but it does help to constrain lithospheric strength in the southern Colorado Plateau region during the Jurassic to Early Cretaceous, prior to tectonic and chemical modification.

4.1. Alternative Uplift Mechanisms

Effective elastic thicknesses >30 km are somewhat uncommon in regions of active rifting and are above the global average for continental lithosphere (McKenzie & Fairhead, 1997; Tesauro et al., 2012). However, the flanks of continental rifts that form in old, cold, peri-cratonic to cratonic lithosphere often have effective elastic thicknesses approaching or exceeding 50 km, including the Baikal rift (30–50 km; van der Beek, 1997), the Transantarctic Mountains rift (ca. 80 km; ten Brink et al., 1997), and parts of the East African Rift (45–80 km; Ebinger et al., 1989, 1991). Other mechanisms besides high effective elastic thickness could produce very broad rift shoulders, but they are considered unlikely. Lithospheric necking of ductile lower crust beneath rift shoulders may cause broad uplift (Chéry et al., 1992; Kooi et al., 1992). Ductile thinning of the lower crust in the Colorado Plateau during the Jurassic to Early Cretaceous has not been previously documented or hypothesized. The Colorado Plateau crust and cratonic lithosphere has been interpreted to have been relatively cold and stable during this time and shallow marine sedimentation (e.g., Mancos Shale) suggests that, apart from the Mogollon Highlands, the area was near or below sea level until the Late Cretaceous (Bond, 1976; DeCelles, 2004).

Mantle flow and thermal isostacy related to mantle flow may also cause uplift and regional tilting. For example, a mantle plume has been proposed to contribute to rift flank uplift in the East African Rift near the Afar triple junction (e.g., Pik et al., 2008). However, no independent evidence exists for the presence of a mantle plume or significant mantle upwelling in the Mogollon Highlands area during the Jurassic to Early Cretaceous. Relatively rare, syn-rift basalt sills, dikes, and lava flows are associated with the Bisbee Rift, but the rift system is generally magma poor (Dickinson & Lawton, 2001; Glazner et al., 2008; Lawton & McMillan, 1999; Spencer et al., 2011). Mantle upwelling or dynamic uplift related to mantle flow has been proposed to have uplifted the Colorado Plateau and the Mogollon Highlands during the Laramide Orogeny and during the Neogene (Karlstrom et al., 2008, 2012; Liu & Gurnis, 2010; Moucha et al., 2009; van Wijk et al., 2010). These processes may explain Late Cretaceous to Cenozoic uplift, but cannot explain uplift of the Mogollon Highlands associated with the sub-Dakota unconformity. Likewise, contractional deformation and magmatism associated with the Laramide Orogeny locally thickened the crust (Chapman et al., 2020) and may have uplifted the Mogollon Highlands and produced flexural responses (e.g., Gastil et al., 1992; Karlstrom et al., 2020), but these processes post-date the sub-Dakota unconformity. For example, the transition from rift-related sedimentation (ca. 155–100 Ma) to contraction-related sedimentation (ca. 100–78 Ma) in the McCoy Mountains Formation in southeastern California and western Arizona (Spencer et al., 2011) is younger than the sub-Dakota unconformity and mostly younger than the Dakota Formation that onlaps onto the Mogollon Highlands (Figure 5).

Provenance and paleocurrent data from the Morrison Formation indicate that uplift and erosion of the Mogollon Highlands started during the Late Jurassic (e.g., Dickinson & Gehrels, 2008), around the same time that magmatism in the Jurassic arc (ca. 190–150 Ma) in southeastern California, southern Arizona, and northwestern Mexico was waning (Barth et al., 2008, 2017; Tosdal & Wooden, 2015) (Figures 4 and 5). Cessation of Jurassic arc magmatism and initiation of the Bisbee rift system have been attributed to slab rollback (Bilodeau, 1982; Dickinson & Lawton, 2001; Lawton & McMillan, 1999). Although difficult to test, it is conceivable that mantle upwelling during slab rollback contributed to uplifting the Mogollon

Highlands during the Jurassic. The central U.S. Cordillera experienced surface uplift during the Paleogene, following roll-back of the Farallon slab (Cassel et al., 2018), which may be analogous to the Jurassic arc; however, the uplifted region in the central U.S. Cordillera was much broader than the Mogollon Highlands and uplift was accompanied by widespread magmatism (i.e., the mid-Cenozoic ignimbrite flare up). Widespread magmatism has also been associated with Neogene to present slab rollback in the central Andes (e.g., de Silva & Kay, 2018). Analogous magmatic activity did not occur in the southern U.S. Cordillera during the Late Jurassic to Early Cretaceous. Hence, we favor flexural uplift of the northern Bisbee rift shoulder to explain the sub-Dakota unconformity in the Mogollon Highlands area.

4.2. Deposition in a Flexural Trough

One of the interesting implications of this study is that the southern part of the Morrison Formation may have been deposited in a flexural trough related to the uplifted Bisbee rift shoulder (Figures 2 and 7), which is consistent with paleocurrent and provenance data linking the southern Morrison basin to the Mogollon Highlands. Basins formed in rift-related flexural troughs are uncommon, or at least not widely recognized (e.g., van Balen et al., 1995). Examples include the Kalahari basin associated with the Great Escarpment in southern Africa, the Wilkes basin associated with the west Antarctic rift system, the Manesi, Trichonis, Copais, and Istiea basins associated with the Corinth rift in Greece, and the Estancia basin in the Rio Grande rift (Poulimenos & Doutsos, 1997; Roy et al., 1999; ten Brink & Stern, 1992; van Wijk, Lawrence, & Driscoll, 2008; van Wijk, Van Hunen, & Goes, 2008; Wanke & Wanke, 2007). The relative scarcity of rift-flank flexural trough basins reported in the literature is somewhat surprising considering the likelihood for preservation, particularly in comparison to back-bulge depozones, another type of flexural basin. Recognition of back-bulge depozones in the stratigraphic record has proliferated in the past two decades although flexural subsidence in a back-bulge region is limited to a few 10s of meters and back-bulge deposits are commonly eroded by the laterally migrating forebulge (DeCelles, 2012). Conversely, subsidence in rift-flank flexural trough basins can reach a few 100 s of meters for common values of rift flank uplift (1–4 km) and effective elastic thickness (10–40 km) (Figure 2). Lower values of effective elastic thickness will produce greater flexural subsidence. For example, Roy et al. (1999) estimated as much as 600 m of flexural subsidence in the Estancia basin in the Rio Grande rift with an effective elastic thickness of ~5 km. Rift flanks are also commonly subjected to thermal and isostatic subsidence following rifting that can preserve basin deposits (e.g., Viking graben; Badley et al., 1988; White & McKenzie, 1988). Modeling by Ziegler and Cloetingh (2004) suggests that rift systems are ~65% thermally equilibrated ca. 60 Myr after the end of rifting, which is similar to the difference in age between the (transgressive) lower Dakota Formation on the northern shoulder of the Bisbee rift and the Morrison Formation (Cobban & Hook, 1984; Turner & Peterson, 2004). In any case, spatial fixity of rifts (in contrast to the extreme lateral mobility of thrust belts and their foreland flexural waves) reduces the erosional potential of forebulge uplift.

The Morrison basin is ca. 75–100 m thicker in the Four Corners region of the Colorado Plateau than elsewhere in the Cordilleran foreland basin (Figure 1), which is similar to the maximum amount of subsidence (60–70 m) predicted by our 2D and 3D flexural models (Table 1). Another way to state this is that ca. 75–100 m of the Morrison Formation (up to ~50% of the total thickness) in the Four Corners area cannot be explained by subsidence of a back-bulge depozone alone. The flexural models also predict positive interference between a flexural trough and the Cordilleran back-bulge depozone that may have amplified subsidence in this region. Constructive flexural interference (uplift) between a rift and foreland basin has been proposed for the uplifted shoulder of the Rhine graben and the Alpine foreland basin forebulge (Gutscher et al., 1995). The Morrison basin may be another example of flexural interference. The predicted amount of subsidence is less than the actual thickness (up to 325 m) of the Morrison Formation, with the additional thickness interpreted to be related to aggradation up to a stratigraphic base level and possible dynamic subsidence (Currie, 1998; DeCelles & Currie, 1996). In addition to influencing depositional patterns in the Morrison Formation, the intersection of the Cordilleran thrust belt and the uplifted Bisbee rift shoulder affected the paleogeography of the Western Interior Basin throughout the Cretaceous and resulted in a long-lived embayment, or "bight," in eastern Utah and western Colorado (Van Cappelle et al., 2018).

5. Conclusions

Results of this study indicate that the Mogollon Highlands, interpreted to be the northern uplifted shoulder of the Bisbee segment of the Borderland Rift Belt, experienced 1.5–2.5 km of total uplift during the Late Jurassic to mid-Cretaceous (ca. 145–95), based on assumptions about topographic slope and fluvial gradients. Uplift and erosion of the rift flank during this time are indicated by the regional sub-Dakota unconformity. The Mogollon Highlands may have been uplifted during younger geologic events, like the Laramide Orogeny, but those uplift events are not recorded by the sub-Dakota unconformity. A subcrop map of this unconformity and a cross-section, structurally restored to Late Jurassic time, were constructed and used to model deformation of the northern Bisbee rift shoulder in 2D and 3D using both analytical and numerical methods. The geometry of the rift shoulder can be reproduced by flexural models with geologically reasonable values for vertical loads and flexural rigidity. Although the magnitude of the vertical loads is not well constrained—because the total amount of rift flank uplift is not well constrained—the model estimates for flexural rigidity are geologically significant. Our modeling indicates an effective elastic thickness for the Colorado Plateau region of 55 ± 5 km during the Late Jurassic, within uncertainty of previous estimates based on flexural modeling of the Cordilleran foreland basin (DeCelles, 2004). The results suggest that the flexural rigidity of the lithosphere in the Colorado Plateau has decreased from the Late Jurassic to the present.

In addition to explaining the sub-Dakota unconformity in the southern Colorado Plateau, flexural modeling of the Bisbee rift shoulder predicts subsidence in a flexural trough in the Four Corners region. The best-fit parameters in the 2D and 3D models suggest up to ca. 70 m of subsidence related to rift-flank flexure alone. Constructive interference between the flexural trough and the flexural back-bulge depozone in the foreland basin system may have amplified subsidence in this area. Increased flexure-related subsidence may help to explain the anomalous thickness of the Morrison Formation in the Four Corners area, which is 75–100 m thicker than elsewhere in the Cordilleran foreland basin. The study highlights a rare example of a flexural trough basin and an even rarer example of flexural interference between competing tectonic elements in an orogenic system. It also emphasizes the importance of considering along-strike changes in the tectonic configuration of Cordilleran systems and how they can influence foreland basin depositional patterns.

Data Availability Statement

Data analyzed in this study include isopach maps of the Morrison Formation, available through Craig et al. (1955) and Dam et al. (1990). The subcrop paleogeologic map of the sub-Cretaceous unconformity was constructed using data available through the USGS National Geologic Map Database (https://ngmdb.usgs.gov/ngmdb/ngmdb_home.html), which includes geologic maps published by the USGS, Nevada Bureau of Mines and Geology, Utah Geological Survey, Colorado Geological Survey, New Mexico Bureau of Geology and Mineral Resources, and Arizona Geological Survey.

Acknowledgments
The support was provided by National Science Foundation (NSF) Tectonics EAR-1928312 (Chapman) and NSF Tectonics EAR-1919179 (DeCelles). Discussion with Dr. Brian Currie and constructive reviews by Dr. Cari Johnson and Dr. Karl Karlstrom helped improve the manuscript.

References

Anderson, O. J., & Lucas, S. G. (1994). Middle Jurassic stratigraphy, sedimentation and paleogeography in the southern Colorado Plateau and southern High Plains. In Caputo, M. V., Peterson, J. A., & Fraczyk, K. J. (Eds.), *Mesozoic systems of the Rocky Mountain region*. (pp. 299–314), Denver, CO: Rocky Mountain Section of the Society for Sedimentary Geology (SEPM).

Aubrey, W. M. (1989). Mid-Cretaceous alluvial-plain incision related to eustasy, southeastern Colorado Plateau. *Geological Society of America Bulletin*, *101*, 443–449. https://doi.org/10.1130/0016-7606(1989)101<0443:mcapir>2.3.co;2

Badley, M. E., Price, J. D., Dahl, C. R., & Agdestein, T. (1988). The structural evolution of the northern Viking Graben and its bearing upon extensional modes of basin formation. *Journal of the Geological Society*, *145*, 455–472. https://doi.org/10.1144/gsjgs.145.3.0455

Barth, A. P., Wooden, J. L., Howard, K. A., Richards, J. L., Wright, J. E., & Shervais, J. W. (2008). Late Jurassic plutonism in the southwest U.S. Cordillera. In Wright, J. E., & Shervais, J. W. (Eds.), *Ophiolites, Arcs, and Batholiths: A tribute to Cliff Hopson* (Vol. 438, pp. 379–396). Geological Society of America Special Paper. https://doi.org/10.1130/2008.2438(13)

Barth, A. P., Wooden, J. L., Jacobson, C. E., & Probst, K. (2004). U-Pb geochronology and geochemistry of the McCoy Mountains formation, southeastern California: A Cretaceous retroarc foreland basin. *Geological Society of America Bulletin*, *116*, 142–153.

Barth, A. P., Wooden, J. L., Miller, D. M., Howard, K. A., Fox, L. K., Schermer, E. R., & Jacobson, C. E. (2017). Regional and temporal variability of melts during a Cordilleran magma pulse: Age and chemical evolution of the Jurassic arc, eastern Mojave Desert, California. *Geological Society of America Bulletin*, *129*, 429–448. https://doi.org/10.1130/b31550.1

Beaumont, C. (1981). Foreland basins. *Geophysical Journal International*, *65*, 291–329. https://doi.org/10.1111/j.1365-246x.1981.tb02715.x

Bilodeau, W. L. (1982). Tectonic models for Early Cretaceous rifting in southeastern Arizona. *Geology*, *10*, 466–470.

Bilodeau, W. L. (1986). The Mesozoic Mogollon Highlands, Arizona: An Early Cretaceous rift shoulder. *The Journal of Geology*, *94*, 724–735. https://doi.org/10.1086/629077

Bond, G. A. (1976). Evidence for continental subsidence in North America during the Late Cretaceous global submergence. *Geology*, *4*, 557–560. https://doi.org/10.1130/0091-7613(1976)4<557:efcsin>2.0.co;2

Brown, C. D., & Phillips, R. J. (1999). Flexural rift flank uplift at the Rio Grande rift, New Mexico. *Tectonics*, *18*, 1275–1291. https://doi.org/10.1029/1999tc900031

Buck, W. R. (1986). Small-scale convection induced by passive rifting: The cause for uplift of rift shoulders. *Earth and Planetary Science Letters*, *77*, 362–372. https://doi.org/10.1016/0012-821x(86)90146-9

Cadigan, R. A. (1967). Petrology of the Morrison Formation in the Colorado Plateau region. *U.S. Geological Survey Professional Paper*, *556*, 113. https://doi.org/10.3133/pp556

Cardozo, N., & Jordan, T. (2001). Causes of spatially variable tectonic subsidence in the Miocene Bermejo Foreland Basin, Argentina. *Basin Research*, *13*, 335–357. https://doi.org/10.1046/j.0950-091x.2001.00154.x

Cassel, E. J., Smith, M. E., & Jicha, B. R. (2018). The impact of slab rollback on earth's surface: Uplift and extension in the hinterland of the North American Cordillera. *Geophysical Research Letters*, *45*, 10–996. https://doi.org/10.1029/2018gl079887

Catuneanu, O. (2004). Retroarc foreland systems – Evolution through time. *Journal of African Earth Sciences*, *38*, 225–242. https://doi.org/10.1016/j.jafrearsci.2004.01.004

Caylor, E. A., Carrapa, B., Sundell, K., DeCelles, P. G., & Smith, J. M. (2021). Age and deposition of the Fort Crittenden Formation: A window into Late Cretaceous Laramide and Cenozoic tectonics in southeastern Arizona. *Geologic Society of America Bulletin*. https://doi.org/10.1130/B35808.1

Chapman, A. D., Rautela, O., Shields, J., Ducea, M. N., & Saleeby, J. (2019). Fate of the lower lithosphere during shallow-angle subduction: The Laramide example. *Geological Society of America Today*, *30*. https://doi.org/10.1130/GSATG412A.1

Chapman, J. B., Carrapa, B. C., Ballato, P., DeCelles, P. G., Worthington, J., Oimahmadov, I., et al. (2017). Intracontinental subduction beneath the Pamir Mountains: Constraints from thermokinematic modeling of shortening in the Tajik fold-and-thrust belt. *Geological Society of America Bulletin*, *129*, 1450–1471.

Chapman, J. B., Greig, R., & Haxel, G. B. (2020). Geochemical evidence for an orogenic plateau in the southern US and northern Mexican Cordillera during the Laramide orogeny. *Geology*. *48*, 164–168.

Chen, B., Kaban, M. K., El Khrepy, S., & Al-Arifi, N. (2015). Effective elastic thickness of the Arabian plate: Weak shield versus strong platform. *Geophysical Research Letters*, *42*, 3298–3304. https://doi.org/10.1002/2015gl063725

Chéry, J., Lucazeau, F., Daignieres, M., & Vilotte, J.P. (1992). Large uplift of rift flanks: A genetic link with lithospheric rigidity? *Earth and Planetary Science Letters*, *112*, 195–211.

Clinkscales, C. A., & Lawton, T. F. (2018). Mesozoic–Paleogene structural evolution of the southern US Cordillera as revealed in the Little and Big Hatchet Mountains, southwest New Mexico, USA. *Geosphere*, *14*, 162–186. https://doi.org/10.1130/ges01539.1

Cobban, W. A., & Hook, S. C. (1984). Mid Cretaceous molluscan biostratigraphy and paleogeography of southwestern part of Western Interior, United States. In Westerman, C. E. G. (Ed.), *Jurassic-Cretaceous biochronology and paleogeography of North America* (Vol. 27, pp. 257–271). Geological Association of Canada Special Paper.

Craig, L. C., Holmes, C. N., Cadigan, R. A., Freeman, V. L., Mullens, T. E., & Weir, G. W. (1955). Stratigraphy of the Morrison and related formations, Colorado Plateau region: In Contributions to the Geology of Uranium 1953–54. *US Geological Survey Bulletin*, *1009*, 125–168.

Currie, B. S. (1997). Sequence stratigraphy of nonmarine Jurassic–Cretaceous rocks, central Cordilleran foreland-basin system. *Geological Society of America Bulletin*, *109*, 1206–1222. https://doi.org/10.1130/0016-7606(1997)109<1206:ssonjc>2.3.co;2

Currie, B. S. (1998). Upper Jurassic-Lower Cretaceous Morrison and Cedar Mountain formations, NE Utah-NW Colorado; relationships between nonmarine deposition and early Cordilleran foreland-basin development. *Journal of Sedimentary Research*, *68*, 632–652. https://doi.org/10.2110/jsr.68.632

Currie, B. S., McPherson, M. L., Dark, J. P., & Pierson, J. S. (2008). Reservoir characterization of Cretaceous Cedar Mountain and Dakota Formations, southern Uinta Basin, Utah: Year-two report. *Utah Geological Survey Open-File Report*, *516*, 67.

Currie, B. S., McPherson, M. L., Hokanson, W., Pierson, J. S., Homan, M. B., Pyden, T., et al. (2012). Reservoir characterization of the lower Cretaceous Cedar Mountain and Dakota Formation. Northern Uinta Basin, Utah. *Utah Geological Survey Open-File Report*, *597*, 34.

Dam, W. L., Kernodle, J. M., Thorn, C. R., Levings, G. W., & Craigg, S. D. (1990). *Hydrogeology of the Morrison Formation in the San Juan structural basin*. (HA-0720-J, 2 sheets). New Mexico, Arizona, and Utah: U.S. Geological Survey, Hydrologic Investigations Atlas.

Daradich, A., Mitrovica, J. X., Pysklywec, R. N., Willett, S. D., & Forte, A. M. (2003). Mantle flow, dynamic topography, and rift-flank uplift of Arabia. *Geology*, *31*, 901–904. https://doi.org/10.1130/g19661.1

Dávila, F. M., Lithgow-Bertelloni, C., & Giménez, M. (2010). Tectonic and dynamic controls on the topography and subsidence of the Argentine Pampas: The role of the flat slab. *Earth and Planetary Science Letters*, *295*, 187–194. https://doi.org/10.1016/j.epsl.2010.03.039

DeCelles, P. G. (2004). Late Jurassic to Eocene evolution of the Cordilleran thrust belt and foreland basin system, western USA. *American Journal of Science*, *304*, 105–168. https://doi.org/10.2475/ajs.304.2.105

DeCelles, P. G. (2012). Foreland basin systems revisited: Variations in response to tectonic settings. In Busby, C., & Azor, A. (Eds.), *Tectonics of sedimentary basins: Recent advances* (pp. 405–426). Blackwell. https://doi.org/10.1002/9781444347166.ch20

DeCelles, P. G., & Burden, E. T. (1992). Non-marine sedimentation in the overfilled part of the Jurassic-Cretaceous Cordilleran foreland basin: Morrison and Cloverly Formations, central Wyoming, USA. *Basin Research*, *4*, 291–314. https://doi.org/10.1111/j.1365-2117.1992.tb00050.x

DeCelles, P. G., & Currie, B. S. (1996). Long-term sediment accumulation in the Middle Jurassic–early Eocene Cordilleran retroarc foreland-basin system. *Geology*, *24*, 591–594. https://doi.org/10.1130/0091-7613(1996)024<0591:ltsait>2.3.co;2

DeCelles, P. G., & Giles, K. A. (1996). Foreland basin systems. *Basin Research*, *8*, 105–123. https://doi.org/10.1046/j.1365-2117.1996.01491.x

DeCelles, P. G., & Horton, B. K. (2003). Early to middle Tertiary foreland basin development and the history of Andean crustal shortening in Bolivia. *Geological Society of America Bulletin*, *115*, 58–77. https://doi.org/10.1130/0016-7606(2003)115<0058:etmtfb>2.0.co;2

Demko, T. M., Currie, B. S., & Nicoll, K. A. (2004). Regional paleoclimatic and stratigraphic implications of paleosols and fluvial/overbank architecture in the Morrison Formation (Upper Jurassic), Western Interior, USA. *Sedimentary Geology*, *167*, 115–135. https://doi.org/10.1016/j.sedgeo.2004.01.003

de Silva, S. L., & Kay, S. M. (2018). Turning up the heat: High-flux magmatism in the Central Andes. *Elements: Elements*, *14*, 245–250. https://doi.org/10.2138/gselements.14.4.245

Dickinson, W. R. (2013). Rejection of the lake spillover model for initial incision of the Grand Canyon, and discussion of alternatives. *Geosphere*, *9*, 1–20. https://doi.org/10.1130/ges00839.1

Dickinson, W. R., Fiorillo, A. R., Hall, D. L., Monreal, R., Potochnik, A. R., Swift, P. N., et al. (1989). Cretaceous strata of southern Arizona. *Geologic evolution of Arizona: Arizona Geological Society Digest*, *17*, 447–462.

Dickinson, W. R., & Gehrels, G. E. (2008). Sediment delivery to the Cordilleran foreland basin: Insights from U-Pb ages of detrital zircons in Upper Jurassic and Cretaceous strata of the Colorado Plateau. *American Journal of Science*, *308*, 1041–1082.
Dickinson, W. R., & Lawton, T. F. (2001). Tectonic setting and sandstone petrofacies of the Bisbee basin (USA–Mexico). *Journal of South American Earth Sciences*, *14*, 475–504. https://doi.org/10.1016/s0895-9811(01)00046-3
Eaton, G. P. (2008). Epeirogeny in the Southern Rocky Mountains region: Evidence and origin. *Geosphere*, *4*, 764–784. https://doi.org/10.1130/ges00149.1
Ebinger, C. J., Bechtel, T. D., Forsyth, D. W., & Bowin, C. O. (1989). Effective elastic plate thickness beneath the East African and Afar plateaus and dynamic compensation of the uplifts. *Journal of Geophysical Research*, *94*, 2883–2901. https://doi.org/10.1029/jb094ib03p02883
Ebinger, C. J., Karner, G. D., & Weissel, J. K. (1991). Mechanical strength of extended continental lithosphere: Constraints from the western rift system, East Africa. *Tectonics*, *10*, 1239–1256. https://doi.org/10.1029/91tc00579
Feucht, D. W., Sheehan, A. F., & Bedrosian, P. A. (2017). Magnetotelluric imaging of lower crustal melt and lithospheric hydration in the Rocky Mountain Front transition zone, Colorado, USA. *Journal of Geophysical Research: Solid Earth*, *22*, 9489–9510. https://doi.org/10.1002/2017jb014474
Fuentes, F., DeCelles, P. G., & Gehrels, G. E. (2009). Jurassic onset of foreland basin deposition in northwestern Montana, USA: Implications for along-strike synchroneity of Cordilleran orogenic activity. *Geology*, *37*, 379–382. https://doi.org/10.1130/g25557a.1
Gastil, G., Wracher, M., Strand, G., Lee Kear, L., Eley, D., Chapman, D., & Anderson, C. (1992). The tectonic history of the southwestern United States and Sonora, Mexico, during the past 100 My. *Tectonics*, *11*, 990–997. https://doi.org/10.1029/92tc00596
Glazner, A. F., Carl, B. S., Coleman, D. S., Miller, J. S., & Bartley, J. M. (2008). Chemical variability and the composite nature of dikes from the Jurassic Independence dike swarm, eastern California. In Wright, J. E., & Shervais, J. W. (Eds.), *Ophiolites, Arcs, and Batholiths: A tribute to Cliff Hopson*. (pp. 455–480). Geological Society of America special Paper 438. https://doi.org/10.1130/2008.2438(16)
González-León, C. M., Valencia, V. A., Lawton, T. F., Amato, J. M., Gehrels, G. E., Leggett, W. J., et al. (2009). The Lower Mesozoic record of detrital zircon U-Pb geochronology of Sonora, México, and its paleogeographic implications. *Revista Mexicana de Ciencias Geológicas*, *26*, 301–314.
Gurnis, M. (1992). Rapid continental subsidence following the initiation and evolution of subduction. *Science*, *255*, 1556–1558. https://doi.org/10.1126/science.255.5051.1556
Gutscher, M. A. (1995). Crustal structure and dynamics in the Rhine Graben and the Alpine foreland. *Geophysical Journal International*, *122*, 617–636. https://doi.org/10.1111/j.1365-246x.1995.tb07016.x
Hack, J. T. (1975). Dynamic equilibrium and landscape evolution. In Melhorn, W., & Flemal, R. (Eds.), *Theories of landform development*. (pp. 91–102). Geomorphogy, State University of New York, Binghamton.
Hansley, P. L. (1986). Relationship of detrital, nonopaque heavy minerals to diagenesis and provenance of the Morrison Formation, southwestern San Juan Basin, New Mexico. *American Association of Petroleum Geologists Bulletin*, *A179*, 257–276. https://doi.org/10.1306/st22455c16
Heller, P. L., Bowdler, S. S., Chambers, H. P., Coogan, J. C., Hagen, E. S., Shuster, M. W., et al. (1986). Time of initial thrusting in the Sevier orogenic belt, Idaho-Wyoming and Utah. *Geology*, *14*, 388–391. https://doi.org/10.1130/0091-7613(1986)14<388:toitit>2.0.co;2
Heller, P. L., Ratigan, D., Trampush, S., Noda, A., McElroy, B., Drever, J., & Huzurbazar, S. (2015). Origins of bimodal stratigraphy in fluvial deposits: An example from the Morrison Formation (Upper Jurassic), western USA. *Journal of Sedimentary Research*, *85*, 1466–1477. https://doi.org/10.2110/jsr.2015.93
Humphreys, E., Hessler, E., Dueker, K., Farmer, G. L., Erslev, E., & Atwater, T. (2003). How Laramide-age hydration of North American lithosphere by the Farallon slab controlled subsequent activity in the western United States. *International Geology Review*, *45*, 575–595. https://doi.org/10.2747/0020-6814.45.7.575
Jones, C. H., Mahan, K. H., Butcher, L. A., Levandowski, W. B., & Farmer, G. L. (2015). Continental uplift through crustal hydration. *Geology*, *43*, 355–358. https://doi.org/10.1130/g36509.1
Jordan, T. E. (1981). Thrust loads and foreland basin evolution, Cretaceous, western United States. *AAPG Bulletin*, *65*, 2506–2520. https://doi.org/10.1306/03b599f4-16d1-11d7-8645000102c1865d
Karlstrom, K. E., Coblentz, D., Dueker, K., Ouimet, W., Kirby, E., Van Wijk, J., et al. (2012). Mantle-driven dynamic uplift of the Rocky Mountains and Colorado Plateau and its surface response: Toward a unified hypothesis. *Lithosphere*, *4*, 3–22. https://doi.org/10.1130/l150.1
Karlstrom, K. E., Crow, R., Crossey, L. J., Coblentz, D., & Van Wijk, J. W. (2008). Model for tectonically driven incision of the younger than 6 Ma Grand Canyon. *Geology*, *36*, 835–838. https://doi.org/10.1130/g25032a.1
Karlstrom, K. E., Jacobson, C. E., Sundell, K. E., Eyster, A., Blakey, R., Ingersoll, R. V., et al. (2020). Evaluating the Shinumo-Sespe drainage connection: Arguments against the "old" (70–17 Ma) Grand Canyon models for Colorado Plateau drainage evolution. *Geosphere*, *16*, 1425–1456. https://doi.org/10.1130/ges02265.1
Kauffman, E. G., & Caldwell, W. G. E. (1993). The Western Interior Basin in space and time. In *Evolution of the Western Interior Basin*. (pp. 1–30). Geological Association of Canada Special Paper, 39.
Kirsch, M., Paterson, S. R., Wobbe, F., Ardila, A. M. M., Clausen, B. L., & Alasino, P. H. (2016). Temporal histories of Cordilleran continental arcs: Testing models for magmatic episodicity. *American Mineralogist*, *101*, 2133–2154. https://doi.org/10.2138/am-2016-5718
Kluth, C. F. (1982). *Geology and mid-Mesozoic tectonics of the northern Canelo Hills* (p. 245). Tucson, AZ: University of Arizona, Ph.D. Dissertation.
Kooi, H., Cloetingh, S., & Burrus, J. (1992). Lithospheric necking and regional isostasy at extensional basins 1. Subsidence and gravity modeling with an application to the Gulf of Lions margin (SE France). *Journal of Geophysical Research*, *97*, 17553–17571. https://doi.org/10.1029/92jb01377
Kowallis, B. J., Christiansen, E. H., Deino, A. L., Peterson, F., Turner, C. E., Kunk, M. J., & Obradovich, J. D. (1998). The age of the Morrison Formation. *Modern Geology*, *22*, 235–260.
Laskowski, A. K., DeCelles, P. G., & Gehrels, G. E. (2013). Detrital zircon geochronology of Cordilleran retroarc foreland basin strata western North America. *Tectonics*, *32*, 1027–1048. https://doi.org/10.1002/tect.20065
Lawton, T. F., Amato, J. M., Machin, S. E., Gilbert, J. C., & Lucas, S. G. (2020). Transition from Late Jurassic rifting to middle Cretaceous dynamic foreland, southwestern U.S. and northwestern Mexico. *Geological Society of America Bulletin*, *132*, 2489–2516. https://doi.org/10.1130/B35433.1
Lawton, T. F., & McMillan, N. J. (1999). Arc abandonment as a cause for passive continental rifting: Comparison of the Jurassic Mexican Borderland rift and the Cenozoic Rio Grande rift. *Geology*, *27*, 779–782. https://doi.org/10.1130/0091-7613(1999)027<0779:aaaacf>2.3.co;2

Lawton, T. F., Urueña, J. E. R., Solari, L. A., Terrazas, C. T., Juárez-Arriaga, E., & Ortega-Obregón, C. (2018). Provenance of Upper Triassic–Middle Jurassic strata of the Plomosas uplift, east-central Chihuahua, Mexico, and possible sedimentologic connections with Colorado Plateau depositional systems. In Raymond, V, Ingersoll, R. V., Lawton, T. F., & Graham, S. A., (Eds.), *Tectonics, sedimentary basins, and provenance: A Celebration of the Career of William R. Dickinson*. Vol 540: Geological Society of America Special Paper. https://doi.org/10.1130/2018.2540(22)

Levander, A., Schmandt, B., Miller, M. S., Liu, K., Karlstrom, K. E., Crow, R. S., et al. (2011). Continuing Colorado plateau uplift by delamination-style convective lithospheric downwelling. *Nature*, *472*, 461–465. https://doi.org/10.1038/nature10001

Liu, L., & Gurnis, M. (2010). Dynamic subsidence and uplift of the Colorado Plateau. *Geology*, *38*, 663–666. https://doi.org/10.1130/g30624.1

Long, S. P. (2012). Magnitudes and spatial patterns of erosional exhumation in the Sevier hinterland, eastern Nevada and western Utah, USA: Insights from a Paleogene paleogeologic map. *Geosphere*, *8*, 881–901. https://doi.org/10.1130/ges00783.1

Lowry, A. R., Ribe, N. M., & Smith, R. B. (2000). Dynamic elevation of the Cordillera, western United States. *Journal of Geophysical Research*, *105*, 23371–23390. https://doi.org/10.1029/2000jb900182

Ludvigson, G. A., Joeckel, R. M., Gonzalez, L. A., Gulbranson, E. L., Rasbury, E. T., Hunt, G. J., et al. (2010). Correlation of Aptian-Albian carbon isotope excursions in continental strata of the Cretaceous foreland basin, eastern Utah, USA. *Journal of Sedimentary Research*, *80*, 955–974. https://doi.org/10.2110/jsr.2010.086

Maidment, S. C., & Muxworthy, A. (2019). A chronostratigraphic framework for the Upper Jurassic Morrison Formation, western USA. *Journal of Sedimentary Research*, *89*, 1017–1038. https://doi.org/10.2110/jsr.2019.54

Martinod, J., & Davy, P. (1992). Periodic instabilities during compression or extension of the lithosphere 1. Deformation modes from an analytical perturbation method. *Journal of Geophysical Research*, *97*, 1999–2014. https://doi.org/10.1029/91jb02715

Masek, J. G., Isacks, B. L., Fielding, E. J., & Browaeys, J. (1994). Rift flank uplift in Tibet: Evidence for a viscous lower crust. *Tectonics*, *13*(3), 659–667. https://doi.org/10.1029/94tc00452

McKenzie, D., & Fairhead, D. (1997). Estimates of the effective elastic thickness of the continental lithosphere from Bouguer and free air gravity anomalies. *Journal of Geophysical Research*, *102*, 27523–27552. https://doi.org/10.1029/97jb02481

Miall, A. D., & Catuneanu, O. (2019). The Western Interior Basin. In Miall, A. D. (Ed.), *The sedimentary basins of the United States and Canada* (pp. 401–443). Elsevier. https://doi.org/10.1016/b978-0-444-63895-3.00009-7

Miall, A. D., Catuneanu, O., Vakarelov, B. K., & Post, R. (2008). The Western interior basin. In Miall, A. D. (Ed.), *The sedimentary basins of the United States and Canada*. Sedimentary basins of the world (Vol. 5, pp. 329–362). Elsevier. https://doi.org/10.1016/s1874-5997(08)00009-9

Moucha, R., Forte, A. M., Rowley, D. B., Mitrovica, J. X., Simmons, N. A., & Grand, S. P. (2009). Deep mantle forces and the uplift of the Colorado Plateau. *Geophysical Research Letters*, *36*. https://doi.org/10.1029/2009gl039778

Mueller, K., Kier, G., Rockwell, T., & Jones, C. H. (2009). Quaternary rift flank uplift of the Peninsular Ranges in Baja and southern California by removal of mantle lithosphere. *Tectonics*, *28*, TC5003. https://doi.org/10.1029/2007TC002227

Oldow, J. S. (1984). Evolution of a late Mesozoic back-arc fold and thrust belt, northwestern Great Basin, USA. *Tectonophysics*, *102*, 245–274. https://doi.org/10.1016/0040-1951(84)90016-7

Olmstead, G. A., & Young, K. (2000). Late Jurassic ammonites from the northeastern Chiricahua Mountains, southeast Arizona, New Mexico. *Geology*, *22*, 1–7.

Owen, D. E. (1973). Depositional history of the Dakota sandstone, San Juan basin area, New Mexico. In Fassett, J. E. (Ed.), *Cretaceous and tertiary rocks of the southern Colorado Plateau* (pp. 37–51). Four Corners Geological Society Memoir.

Painter, C. S., & Carrapa, B. (2013). Flexural versus dynamic processes of subsidence in the North American Cordillera foreland basin. *Geophysical Research Letters*, *40*, 4249–4253. https://doi.org/10.1002/grl.50831

Painter, C. S., Carrapa, B., DeCelles, P. G., Gehrels, G. E., & Thomson, S. N. (2014). Exhumation of the North American Cordillera revealed by multi-dating of Upper Jurassic–Upper Cretaceous foreland basin deposits. *Geological Society of America Bulletin*, *126*, 1439–1464.

Peterson, C., & Roy, M. (2005). Gravity and flexure models of the San Luis, Albuquerque, and Tularosa Basins in the Rio Grande Rift, New Mexico and southern Colorado: Field Conference Guidebook. *New Mexico Geological Society*, *56*, 105–114.

Pik, R., Marty, B., Carignan, J., Yirgu, G., & Ayalew, T. (2008). Timing of East African Rift development in southern Ethiopia: Implication for mantle plume activity and evolution of topography. *Geology*, *36*, 167–170. https://doi.org/10.1130/g24233a.1

Pipiringos, G. N., & O'Sullivan, R. B. (1978). *Principal unconformities in Triassic and Jurassic rocks, western interior United States—A preliminary survey* (Professional Paper, 1035-A). (p. 29). U.S. Geological Survey.

Plint, A. G., Tyagi, A., McCausland, P. J. A., Krawetz, J. R., Zhang, H., Roca, X., et al. (2012). Dynamic relationship between subsidence, sedimentation, and unconformities in mid-Cretaceous, shallow-marine strata of the western Canada Foreland basin: Links to Cordilleran tectonics. In Busby, C., & Azor, A. (Eds.), *Tectonics of sedimentary basins: Recent advances* (pp. 480–507). Chichester: Wiley-Blackwell. https://doi.org/10.1002/9781444347166.ch24

Poulimenos, G., & Doutsos, T. (1997). Flexural uplift of rift flanks in central Greece. *Tectonics*, *16*, 912–923. https://doi.org/10.1029/97tc01658

Riggs et al, N. R., Mattinson, J. M., & Busby, C. J. (1993). Correlation of Jurassic eolian strata between the magmatic arc and the Colorado Plateau: New U-Pb geochronologic data from southern Arizona. *Geological Society of America Bulletin*, *105*, 1231–1246. https://doi.org/10.1130/0016-7606(1993)105<1231:cojesb>2.3.co;2

Robinson, J. W., & McCabe, P. J. (1997). Sandstone-body and shale-body dimensions in a braided fluvial system: Salt Wash Sandstone Member (Morrison Formation). *AAPG Bulletin*, *81*, 1267–1291.

Roy, M., Karlstrom, K. E., Kelley, S. A., Pazzaglia, F. J., & Cather, S. (1999). Topographic setting of the Rio Grande rift, New Mexico: Assessing the role of flexural "rift-flank uplift" in the Sandia Mountains. In Pazzaglia, F. J., & Lucas, S. G. (Eds.), *Annual Fall Field conference guidebook: New Mexico geological society* (Vol. 50, pp. 167–174). New Mexico Geological Society.

Royse, F., Jr (1993). Case of the phantom foredeep: Early Cretaceous in west-central Utah, *Utah Geology*, (Vol. 21, pp. 133–136). https://doi.org/10.1130/0091-7613(1993)021<0133:cotpfe>2.3.co;2

Seedorff, E., Barton, M. D., Gehrels, G. E., Valencia, V. A., Johnson, D. A., Maher, D. J., et al. (2019). Temporal evolution of the Laramide arc: U-Pb geochronology of plutons associated with porphyry copper mineralization in east-central Arizona: Geologic excursions in southwestern North America. *Geological Society of America Field Guide*, *55*, 369–400.

Şengör, A. M. C. (2011). Continental Rifts. In Gupta, H. K. (Ed.), *Encyclopedia of solid Earth geophysics* (pp. 41–55). Springer.

Sklar, L., & Dietrich, W. E. (1998). River longitudinal profiles and bedrock incision models: Stream power and the influence of sediment supply. *American Geophysical Union Monograph*, *107*, 237–260. https://doi.org/10.1029/gm107p0237

Spencer, J. E., Richard, S. M., Gehrels, G. E., Gleason, J. D., & Dickinson, W. R. (2011). Age and tectonic setting of the Mesozoic McCoy Mountains Formation in western Arizona. *Geological Society of America Bulletin*, *123*, 1258–1274. https://doi.org/10.1130/b30206.1

Sprinkel, D. A., Madsen, S. K., Kirkland, J. I., Waanders, G. L., & Hunt, G. J. (2012). Cedar Mountain and Dakota Formations around Dinosaur National Monument – Evidence of the first incursion of the Cretaceous Western Interior Seaway into Utah. *Utah Geological Survey Special Study*, *143*, 21.

Stern, R. J., & Dickinson, W. R. (2010). The Gulf of Mexico is a Jurassic backarc basin. *Geosphere*, *6*, 739–754. https://doi.org/10.1130/ges00585.1

Stern, T. A., & ten Brink, U. S. (1989). Flexural uplift of the Transantarctic Mountains. *Journal of Geophysical Research*, *94*, 10315–10330. https://doi.org/10.1029/jb094ib08p10315

ten Brink, U. S., Hackney, R. I., Bannister, S., Stern, T. A., & Makovsky, Y. (1997). Uplift of the Transantarctic Mountains and the bedrock beneath the East Antarctic ice sheet. *Journal of Geophysical Research*, *102*, 27603–27621. https://doi.org/10.1029/97jb02483

ten Brink, U., & Stern, T. (1992). Rift flank uplifts and hinterland basins: Comparison of the Transantarctic Mountains with the Great Escarpment of southern Africa. *Journal of Geophysical Research*, *97*, 569–585. https://doi.org/10.1029/91jb02231

Tesauro, M., Kaban, M. K., & Cloetingh, S. A. (2012). Global strength and elastic thickness of the lithosphere. *Global and Planetary Change*, *90*, 51–57. https://doi.org/10.1016/j.gloplacha.2011.12.003

Tikoff, B., & Maxson, J. (2001). Lithospheric buckling of the Laramide foreland during Late Cretaceous and Paleogene western United States. *Rocky Mountain Geology*, *36*, 13–35. https://doi.org/10.2113/gsrocky.36.1.13

Tosdal, R. M., & Wooden, J. L. (2015). Construction of the Jurassic magmatic arc, southeast California and southwest Arizona. *Geological Society of America Special Paper*, *513*, 189–221.

Trujillo, K. C., Foster, J. R., Hunt-Foster, R. K., & Chamberlain, K. R. (2014). A U/Pb age for the Mygatt–Moore quarry, Upper Jurassic Morrison Formation Mesa County, Colorado. *Volumina Jurassica*, *12*, 107–114.

Tschudy, R. H., Tschudy, B. D., & Craig, L. C. (1984). Palynological evaluation of Cedar Mountain and Burro Canyon Formations, Colorado Plateau. *U. S. Geological Survey Professional Paper*, *1281*, 24.

Turcotte, D. L., & Schubert, G. (2002). *Geodynamics* (p. 456). Cambridge University Press.

Turner, C. E., & Fishman, N. S. (1991). Jurassic Lake T'oo'dichi': A large alkaline, saline lake, Morrison Formation, eastern Colorado Plateau. *Geological Society of America Bulletin*, *103*, 538–558. https://doi.org/10.1130/0016-7606(1991)103<0538:jltoda>2.3.co;2

Turner, C. E., & Peterson, F. (2004). Reconstruction of the Upper Jurassic Morrison Formation extinct ecosystem—A synthesis. *Sedimentary Geology*, *167*, 309–355. https://doi.org/10.1016/j.sedgeo.2004.01.009

Turner-Peterson, C. E. (1986). Fluvial sedimentology of a major uranium-bearing sandstone–A study of the Westwater Canyon Member of the Morrison Formation, San Juan Basin, New Mexico. In ChristineTurner-Peterson, E. C. E., Santos, E. S., & Fishman, N. S. (Eds.), *A basin analysis case study: The Morrison Formation, grants uranium region*. (Vol. 22, pp. 47–75). New Mexico: AAPG studies in Geology. https://doi.org/10.1306/st22455c5

Uličný, D. (1999). Sequence stratigraphy of the Dakota Formation (Cenomanian), southern Utah: Interplay of eustasy and tectonics in a foreland basin. *Sedimentology*, *46*, 807–836. https://doi.org/10.1046/j.1365-3091.1999.00252.x

van Balen, R. T., van der Beek, P. A., & Cloetingh, S. A. P. L. (1995). The effect of rift shoulder erosion on stratal patterns at passive margins: Implications for sequence stratigraphy. *Earth and Planetary Science Letters*, *134*, 527–544. https://doi.org/10.1016/0012-821x(95)98955-l

Van Cappelle, M., Hampson, G. J., & Johnson, H. D. (2018). Spatial and temporal evolution of coastal depositional systems and regional depositional process regimes: Campanian Western Interior Seaway. *Journal of Sedimentary Research*, *88*, (873–897). https://doi.org/10.2110/jsr.2018.49

van der Beek, P. (1997). Flank uplift and topography at the central Baikal Rift (SE Siberia): A test of kinematic models for continental extension. *Tectonics*, *16*, 122–136. https://doi.org/10.1029/96tc02686

van der Beek, P., Cloetingh, S., & Andriessen, P. (1994). Mechanisms of extensional basin formation and vertical motions at rift flanks: Constraints from tectonic modelling and fission-track thermochronology. *Earth and Planetary Science Letters*, *121*, 417–433. https://doi.org/10.1016/0012-821x(94)90081-7

van Wijk, J., Van Hunen, J., & Goes, S. (2008). Small-scale convection during continental rifting: Evidence from the Rio Grande rift. *Geology*, *36*, 575–578. https://doi.org/10.1130/g24691a.1

van Wijk, J. W., Baldridge, W. S., Van Hunen, J., Goes, S., Aster, R., Coblentz, D. D., et al. (2010). Small-scale convection at the edge of the Colorado Plateau: Implications for topography, magmatism, and evolution of Proterozoic lithosphere. *Geology*, *38*, 611–614. https://doi.org/10.1130/g31031.1

van Wijk, J. W., Lawrence, J. F., & Driscoll, N. W. (2008). Formation of the Transantarctic Mountains related to extension of the West Antarctic Rift system. *Tectonophysics*, *458*, 117–126. https://doi.org/10.1016/j.tecto.2008.03.009

Villemin, T., Alvarez, F., & Angelier, J. (1986). The Rhinegraben: Extension, subsidence and shoulder uplift. *Tectonophysics*, *128*, 47–59. https://doi.org/10.1016/0040-1951(86)90307-0

Wanke, H., & Wanke, A. (2007). Lithostratigraphy of the Kalahari Group in northeastern Namibia. *Journal of African Earth Sciences*, *48*, 314–328. https://doi.org/10.1016/j.jafrearsci.2007.05.002

Weissel, J. K., & Karner, G. D. (1989). Flexural uplift of rift flanks due to mechanical unloading of the lithosphere during extension. *Journal of Geophysical Research*, *94*, 13919–13950. https://doi.org/10.1029/jb094ib10p13919

Whipple, K. X., & Tucker, G. E. (1999). Dynamics of the stream-power river incision model: Implications for height limits of mountain ranges, landscape response timescales, and research needs. *Journal of Geophysical Research*, *104*, 17661–17674. https://doi.org/10.1029/1999jb900120

White, N., & McKenzie, D. (1988). Formation of the "steer's head" geometry of sedimentary basins by differential stretching of the crust and mantle. *Geology*, *16*, 250–253. https://doi.org/10.1130/0091-7613(1988)016<0250:fotssh>2.3.co;2

Williamson, T. E., Kirkland, J. I., & Lucas, S. G. (1993). Selachians from the Greenhorn Cyclothem ("Middle" Cretaceous: Cenomanian-Turonian), Black Mesa, Arizona, and the paleogeographic distribution of late cretaceous selachians. *Journal of Paleontology*, *67*, 447–474. https://doi.org/10.1017/s002233600003691x

Wyld, S. J. (2002). Structural evolution of a Mesozoic backarc fold-and-thrust belt in the US Cordillera: New evidence from northern Nevada. *Geological Society of America Bulletin*, *114*, 1452–1468. https://doi.org/10.1130/0016-7606(2002)114<1452:seoamb>2.0.co;2

Ziegler, P. A., & Cloetingh, S. (2004). Dynamic processes controlling evolution of rifted basins. *Earth-Science Reviews*, *64*, 1–50. https://doi.org/10.1016/s0012-8252(03)00041-2